



ELSEVIER

Earth and Planetary Science Letters 196 (2002) 147–159

EPSL

www.elsevier.com/locate/epsl

Productivity response in the North Canary Basin to climate changes during the last 250 000 yr: a multi-proxy approach

Ana Moreno^a, Silvia Nave^b, Holger Kuhlmann^c, Miquel Canals^{a,*},
Jordi Targarona^a, Tim Freudenthal^c, Fatima Abrantes^b

^a Grup de Recerca Consolidat en Geociències Marines, Departament d'Estratigrafia, Paleontologia i Geociències Marines, Universitat de Barcelona, Campus de Pedralbes, E-08028 Barcelona, Spain

^b Departamento de Geologia Marinha, Instituto Geologico e Mineiro, P-2720 Alfragide, Portugal

^c Universität Bremen, FB Geowissenschaften, Postfach 33 04 40, D-28359 Bremen, Germany

Received 28 June 2001; received in revised form 29 November 2001; accepted 6 December 2001

Abstract

We present results from the investigation of the primary productivity record over the last 250 kyr in the North Canary Basin (30°N) off Northwest Africa. Two distinct productive systems interfere in this area: the oligotrophic open ocean and the upwelling filament off Cape Ghir, that occasionally carries offshore cool nutrient-rich waters. The following geochemical and micropaleontological paleoproductivity proxies have been used in our study: calcium carbonate, barium excess (Ba_{excess}), total organic carbon (TOC) and diatoms. Time series analysis of these proxies indicates that paleoproductivity in the North Canary Basin underwent important changes following precession and eccentricity cycles. While the precessional signal appears to be mainly related to trade wind strength, superimposed peaks in Ba_{excess} , TOC and diatom records point to large productivity events at Terminations I, II and III. Lowering of the North Atlantic sea surface temperatures by melt water discharges which in turn strengthened the Azores high-pressure center and increased trade wind velocities is postulated as the mechanism to explain the enhancement of the coastal upwelling and associated filaments at terminations. Additionally, the Canary Current may play a role in transmitting cold melt waters and nutrients from higher latitudes to the North Canary Basin. © 2002 Elsevier Science B.V. All rights reserved.

Keywords: deglaciation; continental margin; West Africa; productivity; paleoclimatology; upwelling

1. Introduction

Upwelling is driven by the interaction of along-shore wind stress and surface current that brings

cold and nutrient-rich subthermocline waters and CO_2 to the surface. This process results in high rates of primary production and carbon fixation. Thus, upwelling systems play an important role in global carbon cycle, acting as CO_2 sources and sinks [1]. Stronger upwelling and associated higher productivity were discussed as cause for variations in atmospheric CO_2 contents during the last glacial/interglacial periods [2]. Therefore, investigation of productivity gradients and patterns in

* Corresponding author. Tel.: +34-93-402-13-60;
Fax: +34-93-402-13-40.
E-mail address: miquel@natura.geo.ub.es (M. Canals).

upwelling areas has become a very important issue in global climate reconstructions.

Coastal upwelling is especially intense in eastern boundary currents, the most important regions being NW Africa–Iberia, SW Africa, Peru–Chile and Oregon–California, that account for 80–90% of total new production [3]. Along the northeastern Atlantic, productivity off Iberia and the NW African coast is linked to the trade winds and the Canary Current (CC) systems through the outgrowth of coastal upwelling and upwelling filaments [4]. Thus, the location of the Azores high-pressure center and its pressure gradient are the main forcings behind upwelling intensity and the resulting productivity pattern in both upwelling regions [5].

According to classical paleoproductivity studies, the NW African upwelling was considered the paradigm for glacial high productivity [6]. However, recent high-resolution studies reported a distinct paleoproductivity maximum at terminations off Cape Blanc (20°N) [7,8]. These authors found that productivity was controlled by advection from the shelf and/or offshore shifts of the upwelling cells related to sea level changes. Since these study areas are under the influence of continental margin processes local oceanographic conditions will determine the productivity records [7]. Similar productivity peaks during glacial/interglacial transitions were found in the Portuguese margin at 41°N from diatom abundance, barium and organic carbon records [9]. The mechanisms that could explain these striking productivity events are a matter of debate.

Although many paleoproductivity records have been obtained from the NW African margin, very few of them are from the region north of the Canary Islands. Within the MAST III funded CANIGO (Canary Islands Azores and Gibraltar Observations) Project, paleoproductivity response to climate changes was studied in the North Canary Basin (NCB) (Fig. 1). The intermediate location of the NCB (30°N), between the upwelling off Cape Blanc and the Portuguese margin, allows us to compare new paleoproductivity records in terms of productivity patterns and forcing mechanisms as related to atmospheric and oceanographic changes. In this study, a multi-proxy ap-

proach was carried out in two sediment cores from the hemipelagic environment that record climatically forced productivity changes beyond the direct influence of coastal processes.

2. Present-day situation

The NCB is located off NW Africa, between 28°N and 32°N (Fig. 1). At present, the NCB receives dust transported from NW Africa by two wind systems: the Saharan Air Layer, with dust sources in the southern Sahara and the Sahel, and the trade winds that carry dust from Morocco and the eastern Sahara [10].

As a consequence of the northward displacement of the subtropical high pressure, coastal upwelling occurs at the NCB latitude mainly during summer and fall [4]. A characteristic feature of this coastal upwelling is the presence of a prominent upwelling filament off Cape Ghir that was revealed by satellite imagery [11,12] and CTD surveys [13]. The filament structure was modelled in both the temperature and velocity fields showing that it carries nutrient-rich cool water offshore out beyond 13°W [14]. Several studies in the NCB area have shown that Cape Ghir filament growth appears to be forced by favorable high wind stress [11]. However, recent SST satellite images indicate that it may extend further offshore during winter, in coincidence with the late winter/early summer productivity bloom previously described in trap studies [15,16]. An additional factor that might control the strength of the filament is the interaction among the CC and bottom topography [4].

The core sites GeoB 4216-1 (30°37.8'N; 12°23.7'W; 2324 m water depth) and GeoB 5559-2 (31°38.7'N; 13°11.2'W; 3178 m water depth) are located under the influence of the Cape Ghir upwelling filament, in a productivity gradient from the coast to the open ocean. Recent studies in the NCB have shown that the present-day productivity signal of Cape Ghir upwelling filament is transferred through the water column and preserved in surface sediments [17,18]. Therefore, the hemipelagic setting off Cape Ghir holds a strong potential to record climatically induced productivity changes. In addition, the site loca-

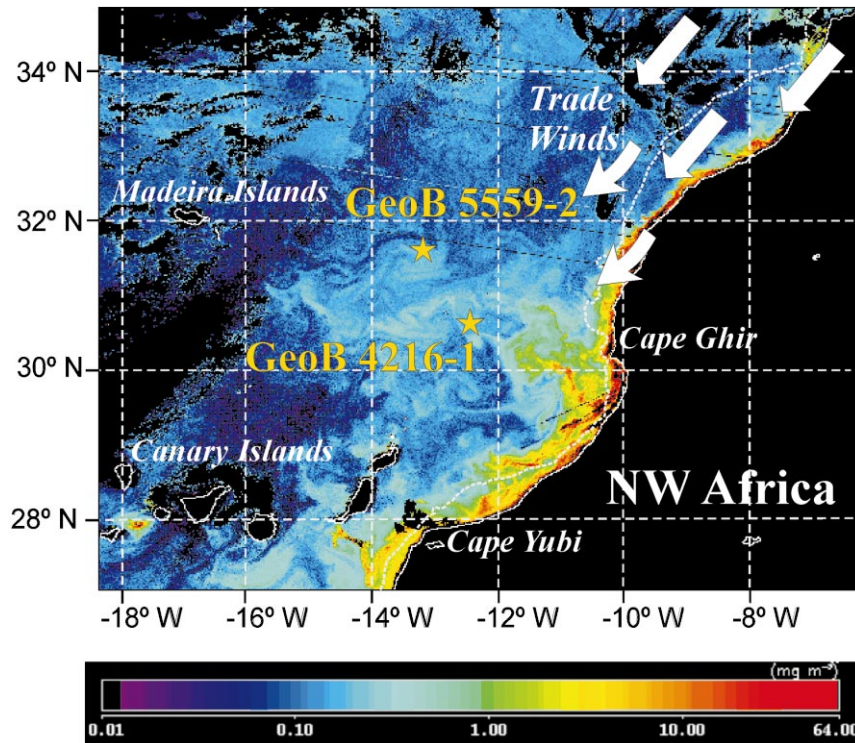


Fig. 1. Surface pigment concentration (mg m^{-3}) in the North Canary Basin as observed by SeaWiFS during an extraordinary Cape Ghir filament event on the 19th March 1998 (processed by R. Davenport). GeoB 4216-1 ($30^{\circ}37.8'N$; $12^{\circ}23.7'W$; 2324 m depth) and GeoB 5559-2 ($31^{\circ}38.7'N$; $13^{\circ}11.2'W$; 3178 m depth) core sites are marked by black stars. The shelf boundary is indicated with a white dashed line.

tions allow us to study the extent of Cape Ghir upwelling filament through the records.

3. Methods

Opening and visual description of the sediment cores was carried out on board (see [19] for core description). Age models based on oxygen isotope stratigraphy for these cores are published [19,20]. Mean sedimentation rates are 2.4 and 4.9 cm/kyr in cores GeoB 5559-2 and GeoB 4216-1, respectively.

3.1. Major and trace elements

Bulk major and trace element contents were analyzed with a sample spacing of 5 cm by means of X-ray fluorescence (XRF). Samples were

ground and homogenized in an agate mortar and prepared for major and trace element determination. For major element measurement, glass discs were processed by melting about 0.3 g of ground bulk sediment with a Li tetra borate flux. For trace element analysis, discs were produced by pressing about 5 g of ground bulk sediment into a briquet, with boric acid backing. Finally, XRF analyses were performed with a Philips PW 2400 sequential wavelength dispersive X-ray spectrometer. Analytical accuracy was checked measuring international standards (GSS-1 to GSS-7) and precision was determined by replicate analyses of samples (0.8 and 4% for major and trace elements, respectively). All standard X-ray fluorescence results were corrected for the contribution and dilution effect of the sea-salt content in the dried sediment [8].

Calcium records obtained by the standard XRF

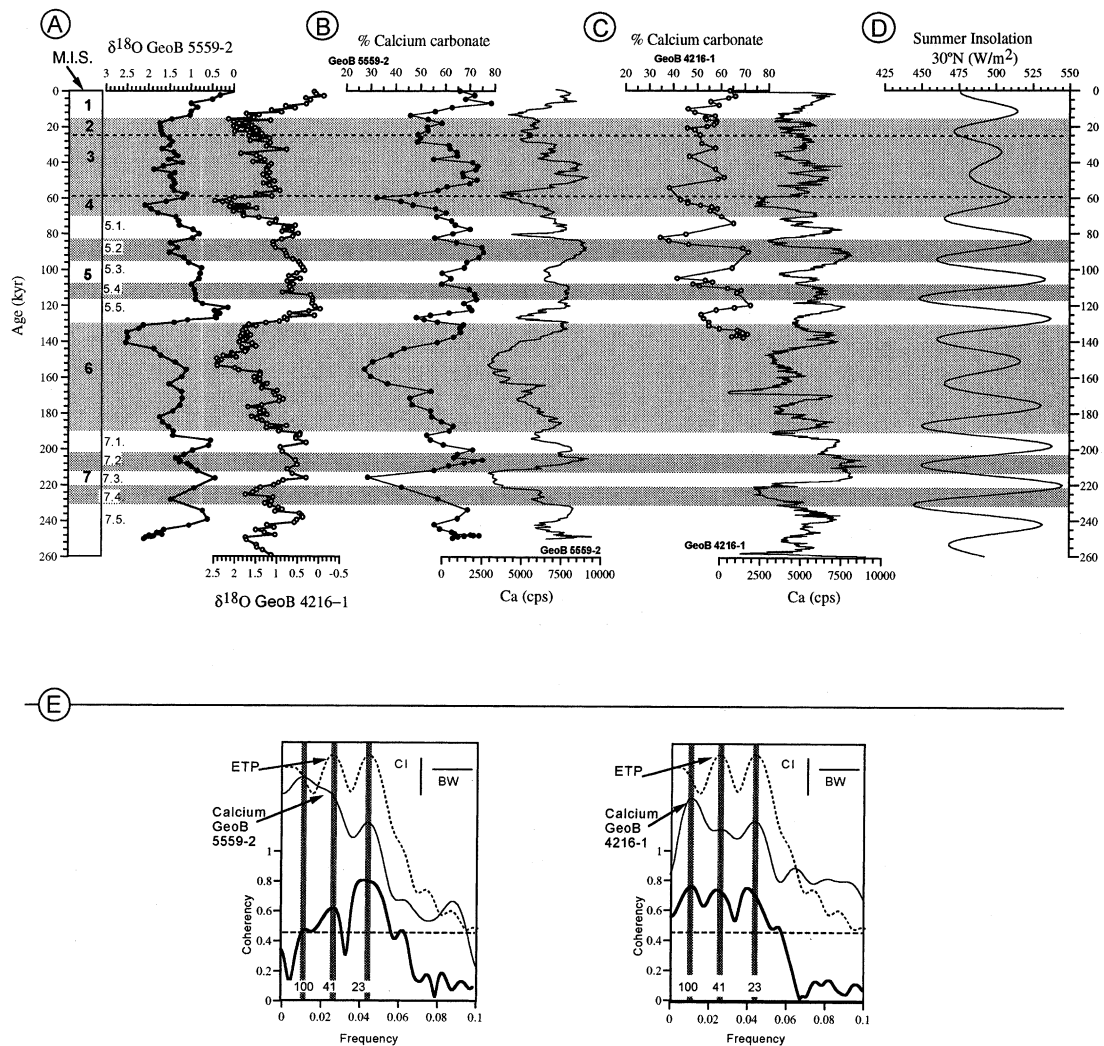


Fig. 2. (A) Oxygen isotope profiles of cores GeoB 5559-2 and GeoB 4216-1 plotted along age (kyr) axis [19,20]. (B) Calcium carbonate (curve with symbols) and Ca intensity from the XRF Scanner (continuous curve) in core GeoB 5559-2 (full symbols) and (C) GeoB 4216-1 (open symbols). Glacial isotopic stages and cold substages are shaded. (D) Boreal summer insolation at 30°N is represented for comparison. (E) Variance spectra of the previous calcium records, expressed as the logarithm of spectral power density vs. frequency in cycles kyr⁻¹ using the Blackman–Tukey method (continuous curve) compared with the spectrum of ETP, eccentricity–tilt–precession combination curve (dashed line). The three main orbital periods of eccentricity (100 kyr), obliquity (41 kyr) and precession (23 kyr) are marked as vertical gray bands. The coherency plot (below, thicker line) indicates what frequency components are shared between the proxies and the ETP curve. An 80% confidence level is set, above which statistical significance in the coherency relationship is considered to exist (this level corresponds in this case to a coherency of 0.048). Bandwidth (BW) and 80% confidence interval (CI) are indicated with short horizontal and vertical segments, respectively.

technique were compared with those achieved at 1 cm interval by means of the XRF core scanner at the Geosciences Department of the University of Bremen. The central sensor unit consists of a

molybdenum X-ray source (3–50 kV), a Peltier-cooled PSI detector (KEVEX[™]) with 125 μm beryllium window and a multichannel analyzer with a 20 eV spectral resolution. The system configu-

ration (X-ray tube energy, detector sensibility) at the University of Bremen allows the analyses of elements from K (atomic no. 19) to Sr (atomic no. 38) (X-ray tube voltage: 20 kV). Each measurement took place over a 1 cm² area and we used 30 s count time and an X-ray current of 0.087 mA. The KEVEX software Toolbox processes the acquired XRF spectrum for each measurement. Background subtraction, sum-peak and escape-peak correction, deconvolution, and peak integration are successively applied. The resulting data are element intensities in counts per second.

Total carbonate content was calculated from the total Ca concentration using a correction for clay-derived Ca, which was established for carbonate-rich sediments: $\text{CaCO}_3 = 2.5(\text{Ca}_{\text{TOT}} - (\text{Ca}/\text{Al}_{\text{clay}} \times \text{Al}_{\text{TOT}}))$; where $\text{Ca}/\text{Al}_{\text{clay}}$ is 0.345 [21].

3.2. Organic carbon

Total carbon was analyzed using a LECO CS-244 at the University of Bremen. Total organic carbon (TOC) was measured after removing the carbonate with 6 M HCl and heating at 80°C. The loss of acid-soluble organic carbon was negligible. Precision was determined by replicate analyses and it was better than 3%.

3.3. Diatoms

While for core GeoB 5559-2 diatoms were counted for the entire length of the core, in core GeoB 4216-1 diatoms were only studied for the two termination intervals. Presence of diatoms

was investigated by smear-slide analysis. In samples where diatoms were present, 2 cm³ of fresh sediment were treated according to the method described in Fenner et al. [22]. Four slides were prepared from each sample using the evaporation tray method [23] and mounted with Permount medium. Diatoms were counted in three of the four prepared slides.

4. Results

4.1. Calcium carbonate

Calcium and carbonate values display the same general trends and amplitudes in both cores (Fig. 2). Higher contents are recorded during the cold periods of interglacial stages and at Stage 3, and tend to correlate with lower values of summer insolation at 30°N.

The cyclicity observed in the records was analyzed by means of power spectra calculations (Fig. 2 and Table 1). Spectral analysis and coherence with the eccentricity–tilt–precession (ETP) combination curve show that both records are dominated by precession and eccentricity cyclicities. Higher values in these proxy records are found during summer insolation minima, which corresponds to maxima in the precessional index (Table 1).

4.2. Barium excess

In order to assess the amount of barium in core GeoB 5559-2 that is present as biogenic barite, we

Table 1
Correlation and phase angle of the studied proxies in cores GeoB 5559-2 and GeoB 4216-1 with respect to ETP

Period (kyr)	SPECMAP	Ca (GeoB 5559-2)	Ca (GeoB 4216-1)	Ba _{excess}	TOC (GeoB 5559-2)	TOC (GeoB 4216-1)
Correlation						
100	0.92	0.42	0.75	0.72	0.77	0.89
41	0.86	0.60	0.74	0.48	0.46	0.75
23	0.92	0.80	0.71	0.70	0.38	0.91
Phase angle						
100	−173 ± 10°	–	3 ± 17°	−135 ± 20°	−175 ± 17°	−145 ± 12°
41	−104 ± 13°	68.4 ± 27°	51 ± 18°	–	–	−80 ± 23°
23	−89 ± 10°	−143 ± 15°	162 ± 20°	−9 ± 21°	–	−40 ± 11°

Maximum ice volume ($\delta^{18}\text{O}$) is based on the SPECMAP curve. $\delta^{18}\text{O}$ values refer to measurements in core GeoB 5559-2. Phase angle is shown for selected proxies (coherency with ETP higher than 0.6 at the 80% of confidence).

corrected the total barium for the non-biogenic portion. In this paper, we refer to this fraction as barium excess (Ba_{excess}). As calculation of Ba_{excess} is still a matter of debate, we have compared the results from four different approaches [24–27]. Given that both barium values and trends are independent of the approach used, we selected the Ba_{excess} determined following Gingele et al. [27] calculations since this method allows to correct the barium included in carbonates, a major component in our sediments.

Ba_{excess} estimations for core GeoB 5559-2 show a pattern marked by an increase in contents, up to

three times the background values, at Terminations I, II and III (Fig. 3A). Smaller peaks are also observed at 38, 60, 107 and 220 kyr. Strong increases in the Ba/Al ratio during terminations were also found in core GeoB 4216-1 (Kasten and Freudenthal, in preparation). In core GeoB 4216-1 Ba/Al values are higher than in core GeoB 5559-2 (i.e. 325 vs. 180.8 at Termination I and 327.8 vs. 211.8 at Termination II) pointing to higher productivity at site GeoB 4216-1 or/and higher degree of barium preservation (Table 2). Ba/Al values were slightly higher in Termination II than in Termination I in both cores. The eccen-

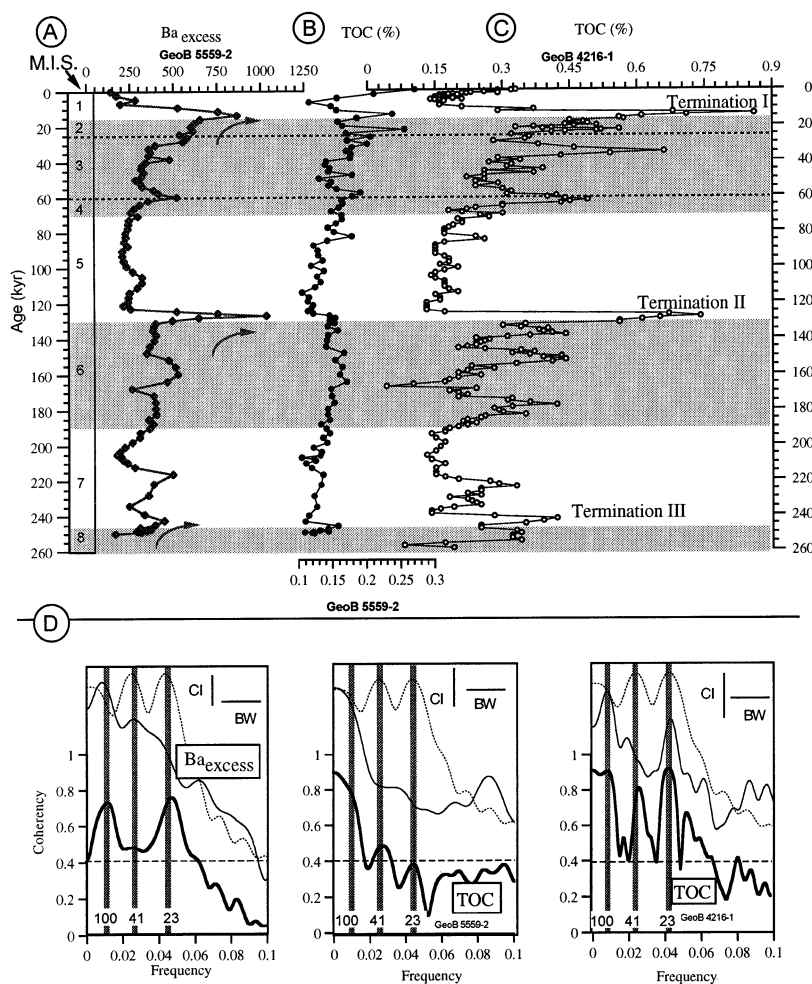


Fig. 3. (A) Ba_{excess} (ppm) record in core GeoB 5559-2 and TOC (%) records in cores GeoB 5559-2 (B) and GeoB 4216-1 (C). Note that both cores are plotted with the same horizontal scale. Glacial periods are shaded and Terminations I, II and III are indicated by arrows. (D) Variance spectra of the previous core profiles (cf. Fig. 2E caption for full explanation).

tricity cycle (100 kyr) dominates the spectral analysis of the Ba_{excess} record (Fig. 3D). Coherence with ETP is highest at the eccentricity and precession parameters while the obliquity signal is not as significant (Table 1).

4.3. Total organic carbon

TOC content is low in the studied cores, ranging from 0.1 up to 0.24% in core GeoB 5559-2 and from 0.1 to 0.9% in core GeoB 4216-1 (Fig. 3B and C). Consistent with the barium results (Table 2), highest TOC values are found at glacial–interglacial transitions in core GeoB 4216-1. However, the TOC record from site GeoB 5559-2 does not follow the Ba_{excess} trend. The spectral analysis of the TOC record does not show any significant cyclicity for core GeoB 5559-2 but re-

Table 2

Comparison of Ba/Al values from GeoB 5559-2 and GeoB 4216-1 cores at Terminations I and II

Event	Ba/Al (GeoB 4216-1)	Ba/Al (GeoB 5559-2)
Termination I	325	180.8
Termination II	327	211.8

veals a clear 100-kyr and 23-kyr cyclicity in core GeoB 4216-1 (Fig. 3D).

4.4. Diatoms

In core GeoB 5559-2 diatoms are found between 10 and 40 kyr while diatom accumulation rate (DAR) shows three distinct peaks at 38, 28 and 18 kyr (Fig. 4). One order of magnitude higher DAR is found at site GeoB 4216-1. The most

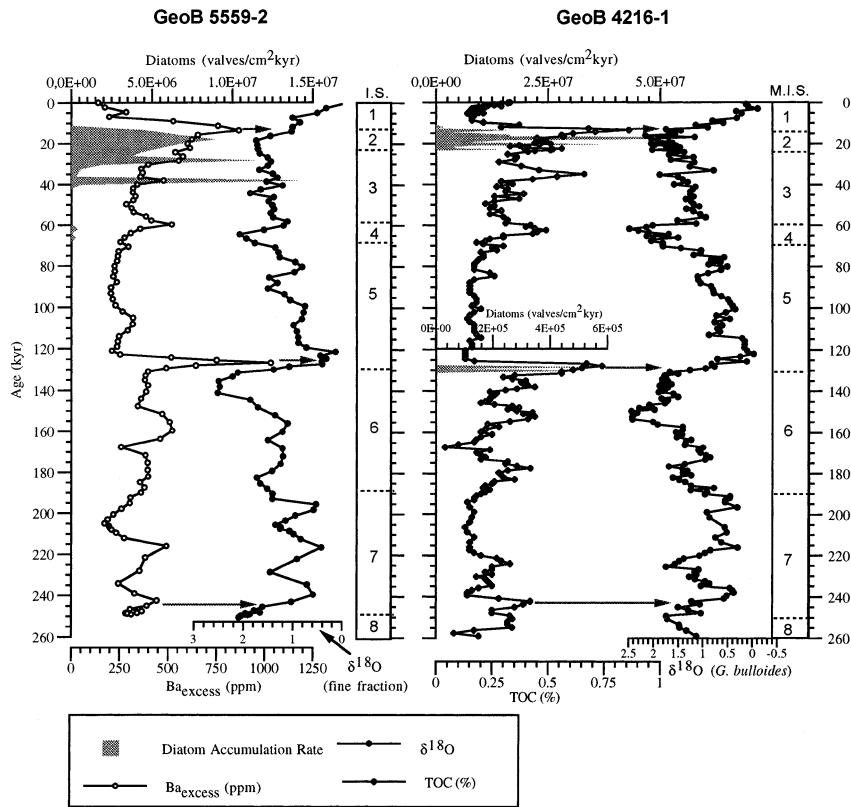


Fig. 4. Diatom accumulation rates (DAR), and oxygen isotope records in cores GeoB 5559-2 and GeoB 4216-1. A different x-scale for DAR at Termination II in core GeoB 4216-1 is used. Ba_{excess} (ppm) and TOC (%) are plotted for comparison. Terminations are indicated with arrows.

common diatom is *Chaetoceros*, a genus that thrives in coastal upwelling waters.

5. Discussion

5.1. Productivity vs. preservation

The original productivity signal might be modified by a variety of processes that include dilution by eolian dust, dissolution and diagenesis. These are considered below for the set of proxies used in the present study.

5.1.1. Calcium carbonate records

According to Henderiks et al. [28] dissolution should have a minor impact on carbonate variability in the NCB context and well-preserved carbonate records are expected in our cores. However, dissolution of sediment carbonate can occur even if the overlying water is saturated with respect to calcite by CO₂ release during oxic decomposition of organic matter [29]. Since carbonate values are lower during TOC peaks (Figs. 2 and 3 and [20]) increased supralysoclinal dissolution could have occurred during higher TOC periods.

The lowest carbonate values are also coincident with high aluminum content and coarse grain size [19]; therefore, dilution by an irregular supply of eolian dust should also be considered as proposed by Matthewson et al. [30] and Shimmield et al. [31] for whom dilution by aeolian dust is the dominant control on carbonate content in the NW African margin. Since our carbonate profiles mirror dust records, and after comparison with other carbonate records [30,31] in the NW African margin, we propose that dilution by non-carbonate material is the most likely process controlling carbonate content variations in the NCB. Calculation of carbonate fluxes to avoid dilution effects has not proved to be useful in this case mainly due to the error margin inherent to the age model construction [19,20]. As a result, we conclude that no reliable paleoproductivity signal can be inferred from the carbonate records in the two studied cores.

5.1.2. Barium excess record

Several studies have established a link between Ba_{excess} and high TOC contents in marine sediments underlying highly productive areas [25]. However, peaks of Ba_{excess} could result from dissolution of barite and subsequent reprecipitation as a diagenetic front under sulfate-depleted environments [32]. This would lead to the formation of Ba_{excess} peaks that are unrelated to productivity. However, according to pore water data, these conditions were not observed in this region [33]. In addition, since Ba and TOC behave differently under oxic or anoxic conditions and since their records are very similar in our cores, we therefore conclude that diagenesis had no significant effects on Ba_{excess}. Consequently, this proxy can be used as a reliable paleoproductivity indicator in the NCB.

5.1.3. Organic carbon records

Prior to assessing past marine carbon fluxes, the contribution of terrigenous to total organic carbon was investigated. On the basis of the C/N ratio, δ¹³C_{org} and δ¹⁵N values in cores from the NCB, Freudenthal et al. [20] concluded that marine organic matter dominates the records.

The proportion of organic matter that becomes preserved in marine sediments depends on primary production, water depth, sedimentation rate and sedimentary redox environment [34]. Differences in TOC contents in the two studied records can be attributed mainly to distinct rates of primary production at the two sites. The proximity to coastal upwelling and the fact that GeoB 4216-1 is below the direct influence of Cape Ghir upwelling filament (Fig. 1) may provide a higher flux of organic matter through the water column at that site. On the contrary, GeoB 5559-2 is influenced by the upwelling filament only when it extends to the core site. The higher contents of Ba_{excess} and diatoms found in core GeoB 4216-1 support this hypothesis (Table 2).

In addition to differences in primary production, the lower sedimentation rates at site GeoB 5559-2 may contribute to reduce preservation of organic carbon by allowing a deeper oxygen penetration [34,35]. Thus, enhanced oxidation could

explain the lack of Ba_{excess} and TOC correlation in core GeoB 5559-2 at terminations.

Kasten et al. [36] have recently proposed that in low sedimentation regimes the action of oxidation fronts induced by changes in deep water conditions leads to a high degradation of TOC. When NADW production was restored after glacial periods aerobic degradation of the organic matter took place. These authors explain the oxidation front development in sediments of the Equatorial Atlantic Ocean in a sequence of three depositional/diagenetic stages (fig. 8 in [36]). First, there was a productivity pulse at glacial/interglacial transition indicated by the increase in Ba_{excess} and TOC. Afterwards, caused by the decreased sedimentation rates and increased oxygen concentration related to NADW production at the onset of interglacial periods, an oxidation front formed with the consequent degradation of TOC. Finally, sediments are recording the productivity event by their Ba_{excess} peak and the redistribution of redox-sensitive elements [36].

After model results, it was demonstrated that there is a correlation between sedimentation rate and TOC preservation in low sedimentation rate regimes [35]. Thus, in low sedimentation areas a higher degradation of organic matter is expected when environmental conditions change, like in a glacial/interglacial transition. The small differences of sedimentation rate between our cores could explain the lack of Ba and TOC correlation at GeoB 5559-2 core since the value of sedimentation rates above 2–3 cm/kyr seems critical in controlling TOC post-depositional oxidation [37]. Therefore, the organic carbon content initially supplied to the sediments could have been degraded at site GeoB 5559-2 by the efficient action of oxidation fronts. In contrast, the initial correlation between Ba and organic carbon in core GeoB 4216-1 still exists because the higher sedimentation rates protected the organic matter from any significant oxidation. It comes then that, while there is a good agreement between Ba_{excess} and TOC records in the relatively high sedimentation regimes, such as site GeoB 4216-1 (Kasten and Freudenthal in preparation) and the Portuguese margin [9], such a correlation is lacking in GeoB 5559-2, a low sedimentation regime.

5.1.4. Diatom records

Since oceans are undersaturated with respect to Si, diatoms can only be preserved in areas where surface circulation leads to significant diatom production [1]. Although the residence time in the water column or at the sediment–water interface control diatom preservation rates, the diatom abundances and assemblage composition found in the surface sediments of the NCB do reflect surface productivity conditions [18].

When compared to Ba_{excess} and TOC records, diatom maximum abundances precede these two proxies in both cores (Fig. 4). This feature might be explained by any processes favoring deeper penetration of Si undersaturated waters. When surficial productivity and opal production decreased after Termination I, the Si content of sediment interstitial waters decreased concurrently, leading to opal dissolution downward. According to the estimations of Peng et al. [38] the penetration depth on these sites could reach over 8 cm in GeoB 4216-1 and 25 cm in GeoB 5559-2. The sharp and almost straight decrease of the top of the diatom record at terminations supports this explanation. Since Ba and TOC records are not influenced by Si reduction in pore waters, the differences between the diatom, Ba_{excess} and TOC signals could be explained.

At Termination II diatoms were found only in core GeoB 4216-1. This fact could only be explained either by an enhanced primary production at this site because of the higher influence of the Cape Ghir upwelling filament, or by diatom preservation conditions. Terminations are intervals of increased melt water discharge into the ocean. Under this scenario, the lower density of surface ocean waters would reduce NADW production. Thus, deep nutrient-rich southern ocean waters can easily spread northwards [39,40]. However, the higher DAR recorded in the shallower core, GeoB 4216-1, from 2324 m depth, points to primary productivity variations between the two sites, as pointed out in section 2, as the determinant factor.

We then accept Ba_{excess} , TOC and DAR records as reliable paleoproductivity proxies in the NCB and the analysis of their temporal patterns of variation must be particularly useful to infer the

mechanisms that influenced paleoproductivity variations.

5.2. Productivity peaks at terminations

At low latitudes paleoproductivity records are mainly dominated by the 23-kyr precession cycle [41]. In our cores, both Ba_{excess} and TOC records correlate with minima in the precessional index (Table 1). This is in agreement with the pattern of grain size and geochemical parameters previously reported for the same cores [19,20]. It was subsequently proposed that the trade wind system was stronger at times of minima in the precessional index resulting in stronger upwelling in the NCB region [19]. However, this precession-driven mechanism does not explain the large productivity peaks recorded at terminations by Ba_{excess} , TOC and diatoms.

Several hypothesis could be then considered. The first refers to variations in NADW formation and associated penetration of southern waters to the NCB. It has been shown that terminations are intervals where maxima in boreal summer insolation, rapid ice-sheet melting and fast rates of sea level rise concur. This favors both a reduction of deep water formation in the North Atlantic and a stronger northern penetration of deep nutrient-rich South Atlantic waters (AABW). However, it is improbable that this mechanism leads to stronger upwelling and higher primary production at the latitude of the NCB because deep waters are not the source of upwelling in this region [6]. Therefore, this hypothesis has to be rejected as the ultimate cause for paleoproductivity peaks at terminations in the NCB.

An alternative second hypothesis could be the varying influence of the Cape Ghir upwelling filament as modulated not only by trade wind strength but also by subaerial/submarine topography and sea level. Since higher rates of sea level rise occur at terminations, the change in subaerial vs. submarine topography might have been the main factor influencing in the remarkable development of the upwelling filament. However, such an explanation, which can be acceptable for local settings and coastal areas, cannot account for similar productivity records observed in far dis-

tant areas, such as the open Equatorial Atlantic Ocean [36].

A third and final hypothesis results from the combination of oceanographic and atmospheric mechanisms. Southward advection of cold surface water by the intermediation of the CC was suggested as the main pathway to transfer the high-latitude climate signal to the eastern tropical Atlantic [42]. This water mass would bring nutrients and may then increase productivity all along the NW African margin. Some authors suggested that the re-establishment of the CC system could cause the higher productivity events recorded at terminations [9,43]. This reasoning deserves attention when trying to explain the productivity peaks found in GeoB 5559-2 and GeoB 4216-1. Overpeck et al. [44] proposed, and tested using general circulation models, that the lowering of North Atlantic SST by glacial melt water releases during deglaciation strengthened the North Atlantic high-pressure system, thus favoring the enhancement of trade wind velocities. This ocean–wind system connection can be explained taking into account the higher thermal difference between land and sea that was reached during terminations. This temperature contrast may modulate the Azores high-pressure intensity leading to an enhancement of the trade wind system. This hypothesis of a coupled tropical/high-latitude North Atlantic climate system operating during the last deglaciation is, in addition, supported by records from various tropical records [45–47]. Therefore, high-latitude low SST anomalies at terminations can enhance trade winds and thereby explain productivity events observed in the areas located under their influence.

A similar hypothesis of stronger winds at terminations has been invoked to explain the increments of *Pinus* and pollen from dry and steppe-type formations at the 2/1 oxygen isotope transition found off Northwest Africa [48,49] and would also account for the grain size increases at Terminations I, II and III observed in the studied cores [19]. Scanning electron microscope (SEM) observation of grains from Termination I samples shows rounded edges and impact marks in the particles surface (Fig. 5), features which are common in wind-borne particles [50]. The large

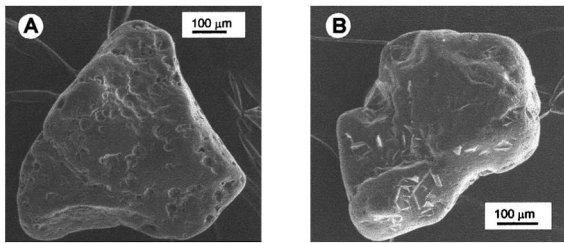


Fig. 5. Scanning electron microscopy (SEM) microphotographs of eolian particles from sediments located at 28 cm depth (Termination I) in core GeoB 5559-2. Note their rounded edges and the signals of eolian impacts. (A) Dolomite, (B) Quartz.

size of these particles (up to 600 μm) further strengthens the hypothesis of stronger trade winds at terminations.

6. Conclusions

Carbonate, $\text{Ba}_{\text{excess}}$, TOC and diatom records were produced for two NCB sediment cores in order to infer paleoproductivity variations over the last 250 kyr. After comparison with previously studied dust records [19], we conclude that calcium carbonate records are affected by dilution. In contrast, $\text{Ba}_{\text{excess}}$, TOC and diatom records appear as reliable indicators of paleoproductivity changes. The precessional signal found in these proxies can be related to trade wind variations as a response to insolation changes in tropical latitudes over the last 250 kyr. During times of maximum summer boreal insolation (minima in the precessional index) trade winds were more intense, enhancing water column mixing and therefore, primary productivity in the NCB.

Large peaks of $\text{Ba}_{\text{excess}}$, TOC and diatoms at Terminations I, II and III suggest the operation of an additional non-precessional-driven mechanism. We hypothesize that the large increase in primary productivity found at terminations results from the intensification of the trade wind system. This enhancement of the atmospheric circulation is related to high-latitude processes occurring during deglaciation, that is, lowering of the North Atlantic SST by melt water discharges which in turn induced the strengthening of the Azores

high-pressure center and increased trade wind velocities. This mechanism may also explain the reinforcement of the coastal upwelling and associated filaments, and the productivity pulses recorded at terminations. Additionally, the CC plays a role in transmitting cold melt waters and nutrients from higher latitudes to the NCB.

Acknowledgements

We gratefully acknowledge the officers and crew of the *R/V Meteor* for technical support during the CANIGO cruises (December 1996 and October 1998) and the Scientific-Technical Services (SCT) of the University of Barcelona for their help in laboratory analyses. We thank R. Davenport for processing SeaWiFS data that were supplied by the SeaWiFS Project and the Distributed Active Archive Center, Goddard Space Flight Center, Greenbelt, MD, USA, and Isabel Cacho (University of Barcelona) and Sabine Kasten (University of Bremen) for their useful comments to an earlier version of the manuscript. We thank three anonymous reviewers who commented on a previous draft of the manuscript. The present study was supported by the CANIGO project (MAS3-CT9-0060) and a Comissionat d'Universitats i Recerca fellowship (A.M.). H.K. acknowledges funding from 'Deutsche Forschungsgemeinschaft' (DF, Grant We 922/31-1). GRC Geociències Marines is funded by 'Generalitat de Catalunya' through its excellency research groups program (ref. 1999 SGR-63).[AC]

References

- [1] W.S. Broecker, T.H. Peng, Tracers in the Sea, Eldigio Press, Palisades, NY, 1982.
- [2] W.S. Broecker, G.M. Henderson, The sequence of events surrounding Termination II and their implications for the cause of glacial–interglacial CO_2 changes, *Paleoceanography* 13 (1998) 352–364.
- [3] W.H. Berger, V. Smetacek, G. Wefer, Productivity of the Ocean: Present and Past, Wiley, Chichester, 1989.
- [4] L. Nykjaer, L. Van Camp, Seasonal and interannual variability of coastal upwelling along northwest Africa and Portugal from 1981 to 1991, *J. Geophys. Res.* 99 (1994) 14197–14207.

- [5] E. Mittelstaedt, The upwelling area off northwest Africa: a description of phenomena related to coastal upwelling, *Prog. Oceanogr.* 12 (1983) 307–331.
- [6] M. Sarnthein, J. Thiede, U. Pflaumann, H. Erlenkeuser, D. Fütterer, B. Koopmann, H. Lange, E. Seibold, Atmospheric and oceanic circulation patterns off Northwest Africa during the past 25 million years, in: U. Rad, I. Hinz, M. Sarnthein, E. Seibold (Eds.), *Geology of the Northwest Africa Continental Margin*, Springer, New York, 1982, pp. 547–604.
- [7] P. Bertrand, G.B. Shimmield, P. Martinez, F.E. Grousset, F. Jorissen, M. Paterne, C. Pujol, I. Bouloubassi, P. Buat-Menard, J.-P. Peypouquet, L. Beaufort, M.-A. Sicre, E. Lallier-Verges, J.M. Foster, Y. Ternois, The glacial ocean productivity hypothesis: the importance of regional temporal and spatial studies, *Mar. Geol.* 130 (1996) 1–9.
- [8] P. Martinez, P. Bertrand, G.B. Shimmield, K. Cochran, F. Jorissen, J.M. Foster, M. Dignan, Upwelling intensity and ocean productivity changes off Cape Blanc (northwest Africa) during the last 70 000 years: geochemical and micropalaeontological evidence, *Mar. Geol.* 158 (1999) 57–74.
- [9] J. Thomson, S. Nixon, C. Summerhayes, E.J. Rohling, J. Schönfeld, R. Zahn, P. Grootes, F. Abrantes, L. Gaspar, S. Vaquero, Enhanced productivity on the Iberian margin during glacial/interglacial transitions revealed by barium and diatoms, *J. Geol. Soc. London* 157 (2000) 667–677.
- [10] I. Chiapello, G. Bergametti, B. Chatenet, Origins of African dust transported over the northeastern tropical Atlantic, *J. Geophys. Res.* 102 (1997) 13701–13709.
- [11] L. Van Camp, L. Nykjaer, E. Mittelstaedt, P. Schlittenhardt, Upwelling and boundary circulation off Northwest Africa as depicted by infrared and visible satellite observations, *Prog. Oceanogr.* 26 (1991) 357–402.
- [12] R. Davenport, S. Neuer, A. Hernández-Guerra, M.J. Ruedas, O. Llinas, G. Fischer, G. Wefer, Seasonal and interannual pigment concentration in the Canary Islands region from CZCS data and comparison with observations from the ESTOC, *Int. J. Rem. Sens.* 20 (1999) 1419–1433.
- [13] E. Hagen, C. Zülicke, R. Feistel, Near-surface structures in the Cape Ghir filament off Morocco, *Oceanol. Acta* 19 (1996) 577–597.
- [14] J. Johnson, I. Stevens, A fine resolution model of the eastern North Atlantic between the Azores the Canary Islands and the Gibraltar Strait, *Deep Sea Res.* 47 (2000) 875–899.
- [15] S. Neuer, V. Ratmeyer, R. Davenport, G. Fischer, G. Wefer, Deep water particle flux in the Canary Island region: a seasonal trend in relation to long-term satellite derived pigment data and lateral sources, *Deep Sea Res.* I 44 (1997) 1451–1466.
- [16] C. Sprengel, K.-H. Baumann, S. Neuer, Seasonal and interannual variation of coccolithophore fluxes and species composition in sediment traps north of Gran Canaria (29°N 15°W), *Mar. Micropal.* 39 (2000) 157–178.
- [17] H. Meggers, T. Freudenthal, S. Nave, J. Targarona, F. Abrantes, P. Helmke, R. Davenport, G. Wefer, Assessment of geochemical and micropaleontological sedimentary parameters as proxies of surface water properties in the Canary Islands region, *Deep Sea Res. II (CANIGO Special Issue)* (2002) in press.
- [18] S. Nave, P. Freitas, F. Abrantes, Coastal upwelling in the Canary Island region: spatial variability reflected by the surface sediment diatom record, *Mar. Micropal.* 42 (2001) 1–23.
- [19] A. Moreno, J. Targarona, J. Henderiks, M. Canals, T. Freudenthal, H. Meggers, Orbital forcing of dust supply to the North Canary Basin over the last 250 kyrs, *Quat. Sci. Rev.* 20 (2001) 1327–1339.
- [20] T. Freudenthal, H. Meggers, J. Henderiks, H. Kuhlmann, A. Moreno, G. Wefer, Upwelling intensity and filament activity off Morocco during the last 250 000 years, *Deep Sea Res. II (CANIGO Special Issue)* (2002) in press.
- [21] G.B. Shimmield, R. Mowbray, The inorganic geochemical record of the northwest Arabian Sea: a history of productivity variation over the last 400 kyr from sites 722 and 724, in: W. Prell, N. Niitsuma (Eds.), *Proceedings of the Ocean Drilling Program, Scientific Results 117*, 1991, pp. 409–420.
- [22] J. Fenner, Diatoms in the Eocene and Oligocene Sediments off NW Africa, their Stratigraphic and Paleogeographic Occurrences, University of Kiel, 1982.
- [23] R. Batterbee, A new method for estimating absolute microfossil numbers with special reference to diatoms, *Limnol. Oceanogr.* 18 (1973) 647–653.
- [24] H.J. Rutsch, A. Mangini, G. Bonani, B. Dittrich-Hannen, P.W. Kubik, M. Suter, M. Segl, ¹⁰Be and Ba concentrations in West African sediments trace productivity in the past, *Earth Planet. Sci. Lett.* 133 (1995) 129–143.
- [25] J. Dymond, E. Suess, M. Lyle, Barium in deep-sea sediment a geochemical proxy for paleoproductivity, *Paleoceanography* 7 (1992) 163–181.
- [26] R. Schneider, B. Price, P. Müller, D. Kroon, I. Alexander, Monsoon related variations in Zaire (Congo) sediment load and influence of fluvial silicate supply on marine productivity in the east equatorial Atlantic during the last 200 000 years, *Paleoceanography* 12 (1997) 463–481.
- [27] F. Gingele, A. Dahmke, Discrete barite particles and barium as tracers of paleoproductivity in South Atlantic sediments, *Paleoceanography* 9 (1994) 151–168.
- [28] J. Henderiks, T. Freudenthal, H. Meggers, S. Nave, F. Abrantes, J. Bollmann, H.R. Thierstein, Glacial–interglacial variability of particle accumulation in the Canary Basin: a time-slice approach, *Deep Sea Res. II (CANIGO Special Issue)* (2002) submitted for publication.
- [29] G. Reichert, M. denDulk, H.J. Visser, C.H. vanderWeijden, W.J. Zachariasse, A 225 kyr record of dust supply, paleo productivity, the oxygen minimum zone from the Murray Ridge (northern Arabian Sea), *Paleoceanogr. Palaeoclimatol. Palaeocol.* 134 (1997) 149–169.
- [30] A.P. Matthewson, G.B. Shimmield, D. Kroon, A.E. Fal-

- lick, A 300 kyr high-resolution aridity record of the North African continent, *Paleoceanography* 10 (1995) 677–692.
- [31] G.B. Shimmield, Can sediment geochemistry record changes in coastal upwelling palaeoproductivity? Evidence from northwest Africa and the Arabian Sea, in: C.P. Summerhayes, W.L. Prell, K.C. Emeis (Eds.), *Upwelling Systems: Evolution since the early Miocene*, Geological Society, Special Publication 64, London, 1992.
- [32] S.J. Schenau, M.A. Prins, G.J. De Lange, C. Monnin, Barium accumulation in the Arabian Sea: controls on barite preservation in marine sediments, *Geochim. Cosmochim. Acta* 65 (2001) 1545–1556.
- [33] G. Wefer and cruise participants, Report and preliminary results of METEOR-Cruise M 37/1, Lisbon-Las Palmas, 04.12.1996–23.12.1996, *Berichte, Fachbereich Geowissenschaften, Universität Bremen*, Bremen, 1997.
- [34] C. Rühlemann, P. Müller, R. Schneider, Organic carbon and carbonate as paleoproductivity proxies: examples from high and low productivity areas of the tropical Atlantic, in: G. Fischer, G. Wefer (Eds.), *Use of Proxies in Paleooceanography: Examples from the South Atlantic*, Springer, Berlin, 1999, pp. 1–31.
- [35] R.V. Tyson, Sedimentation rate, dilution, preservation and total organic carbon: some results of a modelling study, *Org. Geochem.* 32 (2001) 333–339.
- [36] S. Kasten, R. Haese, M. Zabel, C. Rühlemann, H. Schulz, Barium peaks at glacial terminations in sediments of the equatorial Atlantic Ocean: relicts of deglacial productivity pulses?, *Chem. Geol.* 175 (2001) 635–651.
- [37] M. Jung, J. Ilmberger, A. Mangini, K.C. Emeis, Why some Mediterranean sapropels survived burn-down (and others did not), *Mar. Geol.* 141 (1997) 51–60.
- [38] T.H. Peng, W.S. Broecker, G. Kipphut, N.J. Shackleton, Benthic mixing in deep sea cores as determined by ^{14}C dating and its implications regarding climate stratigraphy and the fate of fossil fuel CO_2 , in: N. Andersen, A. Malahoff (Eds.), *The Fate of Fossil Fuel CO_2 in the Ocean*, Plenum, New York, 1977.
- [39] J. Adkins, E. Boyle, L. Keigwin, E. Cortijo, Variability of the North Atlantic thermohaline circulation during the last interglacial period, *Nature* 390 (1997) 154–156.
- [40] A. Lototskaya, G.M. Ganssen, The structure of Termination II (penultimate deglaciation and Eemian) in the North Atlantic, *Quat. Sci. Rev.* 18 (1999) 1641–1654.
- [41] L. Beaufort, Y. Lancelot, P. Camberlin, O. Cayre, E. Vincent, F.C. Bassinot, L. Labeyrie, Insolation cycles as a major control of equatorial Indian ocean primary production, *Science* 278 (1997) 1451–1454.
- [42] M. Zhao, N.A.S. Beveridge, N.J. Shackleton, M. Sarnthein, G. Eglinton, Molecular stratigraphy of cores off northwest Africa sea surface temperature history over the last 80 ka, *Paleoceanography* 10 (1995) 661–675.
- [43] P.G. Harris, M. Zhao, A. Rosell-Mele, R. Tiedemann, M. Sarnthein, J.R. Maxwell, Chlorin accumulation rate as a proxy for Quaternary marine primary productivity, *Nature* 383 (1996) 63–65.
- [44] J.T. Overpeck, L.C. Peterson, N. Kipp, J. Imbrie, D. Rind, Climate change in the circum-north Atlantic region during the last deglaciation, *Nature* 338 (1989) 553–557.
- [45] K.A. Hughen, J.T. Overpeck, L.C. Peterson, S. Trumbore, Rapid climate changes in the tropical Atlantic region during the last deglaciation, *Nature* 380 (1996) 51–54.
- [46] F.A. Street-Perrot, R.A. Perrot, Abrupt climate fluctuations in the tropics the influence of Atlantic Ocean circulation, *Nature* 343 (1990) 607–612.
- [47] P. deMenocal, J. Ortiz, T.P. Guilderson, M. Sarnthein, Coherent high- and low-latitude climate variability during the Holocene warm period, *Science* 288 (2000) 2198–2202.
- [48] A.M. Lézine, M. Denèfle, Enhanced anticyclonic circulation in the eastern North Atlantic during cold intervals of the last deglaciation inferred from deep-sea pollen records, *Geology* 25 (1997) 119–122.
- [49] F. Marret, J.L. Turon, Paleohydrology and paleoclimatology off Northwest Africa during the last glacial-interglacial transition and the Holocene: palynological evidences, *Mar. Geol.* 118 (1994) 107–117.
- [50] K. Pye, *Aeolian Dust and Dust Deposits*, Academic Press, London, 1987.